Geomorphology 258 (2016) 58–68

Contents lists available at ScienceDirect

Geomorphology

journal homepage: www.elsevier.com/locate/geomorph

Lithologic controls on valley width and strath terrace formation

Sarah A. Schanz *, David R. Montgomery

Department of Earth and Space Sciences, University of Washington, Seattle, WA 98195, United States

ARTICLE INFO

Article history:
Received 3 December 2015
Received in revised form 20 January 2016
Accepted 25 January 2016
Available online 26 January 2016

Keywords:
Strath terraces
Weathering
Bedrock rivers

ABSTRACT

Valley width and the degree of bedrock river terrace development vary with lithology in the Willapa and Nehalem river basins, Pacific Northwest, USA. Here, we present field-based evidence for the mechanisms by which lithology controls floodplain width and bedrock terrace formation in erosion-resistant and easily friable lithologies. We mapped valley surfaces in both basins, dated straths using radiocarbon, compared valley width versus drainage area for basalt and sedimentary bedrock valleys, and constructed slope-area plots. In the friable sedimentary bedrock, valleys are 2 to 3 times wider, host flights of strath terraces, and have concavity values near 1; whereas the erosion-resistant basalt bedrock forms narrow valleys with poorly developed, localized, or no bedrock terraces and a channel steepness index half that of the friable bedrock and an average channel concavity of about 0.5. The oldest dated strath terrace on the Willapa River, T2, was active for nearly 10,000 years, from 11,265 to 2862 calibrated years before present (cal YBP), whereas the youngest terrace, T1, is Anthropocene in age and recently abandoned. Incision rates derived from terrace ages average 0.32 mm y^{-1} for T2 and 11.47 mm y^{-1} for T1. Our results indicate bedrock weathering properties influence valley width through the creation of a dense fracture network in the friable bedrock that results in high rates of lateral erosion of exposed bedrock banks. Conversely, the erosion-resistant bedrock has concavity values more typical of detachment-limited streams, exhibits a sparse fracture network, and displays evidence for infrequent episodic block erosion and plucking. Lithology thereby plays a direct role on the rates of lateral erosion, influencing valley width and the potential for strath terrace planation and preservation.

1. Introduction

Bedrock, or strath, river terraces are often used to infer rates and styles of tectonic strain (e.g., Merritts et al., 1994; Van der Woerd et al., 1998; Lavé and Avouac, 2000; Cheng et al., 2002; Wegmann and Pazzaglia, 2002; Barnard et al., 2004; Mériaux et al., 2005). A number of modeling studies have assessed the role of climatically-driven changes in sediment supply on strath terrace formation (Hancock and Anderson, 2002; Turowski et al., 2007, 2008; Yanites and Tucker, 2010), and field studies have investigated the controls on the development and preservation of strath terraces (García, 2006; Wohl, 2008; Fuller et al., 2009; Finnegan and Balco, 2013; Larson and Dorn, 2014). Strath terraces form through a combination of lateral planation and vertical incision; when rivers with an alluvial cover migrate across valley bottoms, the underlying bedrock is eroded into a planar surface called a strath (Personius et al., 1993; Wegmann and Pazzaglia, 2002; Fuller et al., 2009; Finnegan and Balco, 2013; Pazzaglia, 2013). As vertical incision rates increase, rivers entrench faster than valleys widen, and the former valley surface is abandoned as a strath terrace. Vertical incision leading to strath formation generally is hypothesized to be caused by external changes: wetter climates and lowered sediment supply (Van der Woerd et al., 1998; Wegmann and Pazzaglia, 2002, 2009; Molin et al., 2012) or lowered base level caused by sea level retreat or tectonic uplift (Merritts et al., 1994). Internal forcings such as meander cutoffs are also found to abandon strath terraces through rapid channel avulsion and the upstream propagation of internally created knickpoints (Finnegan and Dietrich, 2011).

Using observations from basins around the world with different climates, tectonics, and vegetative cover, Montgomery (2004) noted that well-developed, planed-off strath terraces were more extensive in less resistant lithologies such as sandstone and siltstone, whereas poorly developed terraces were more common in more resistant lithologies such as quartzite and basalt. Montgomery (2004) hypothesized the difference in strath prevalence relates to the erosional properties of the bedrock; rocks subject to slaking will rapidly weather when subaerially exposed in the channel banks and thus provide the rapid lateral erosion rates necessary to plane an extensive strath. Stock et al. (2005) and Collins et al. (2016) reported rapid (i.e., 1 to 100 mm y^{-1}) historical erosion and localized development of modern strath terraces along particular river reaches flowing over less resistant lithologies experiencing slaking in Washington State and Taiwan. Lithology is also known to influence the width of bedrock channels (Montgomery and Gran, 2001; Snyder and Kammer, 2008; Wohl, 2008) and the relative rates of channel widening and lowering (Hancock et al., 2011), thereby influencing the planation of straths.

* Corresponding author.
E-mail address: schanzs@uw.edu (S.A. Schanz).

http://dx.doi.org/10.1016/j.geomorph.2016.01.015
0169-555X/

Previous research has thus far focused on the role of lithology in controlling channel width. Here we investigate the role of lithology on strath terrace formation and preservation through its influence on valley width. The valley width reflects the preservation space for strath terraces and is also indicative of a river's ability to laterally planate and form the strath. Do the same processes that control channel width also govern valley width? Specifically, we examine the effect of lithology on spatial patterns of strath terrace preservation and valley width within the Willapa River basin in southwest Washington and the Nehalem River basin in northwest Oregon (Fig. 1), where exposures of basalt and siltstone alternate along the river profiles. We analyze the influence of bedrock properties on valley width, strath terrace presence, and relative rates of vertical and lateral erosion to assess the processes of and lithologic controls on strath terrace formation.

2. Channel erosion

Lateral and vertical incision rates are set by in-channel erosion rates and processes, which in turn are dominated by bedrock lithology, sediment supply, and water discharge (Hancock and Anderson, 2002; Pazzaglia, 2013). Vertical stream channel erosion is often expressed as a function of these factors:

$$E = K\,S^m A^n \tag{1}$$

where E is the erosion rate, S is channel slope, A is drainage area as a proxy for water discharge, and K, m, and n are empirical constants that relate to bedrock erodibility, climate, incisional processes, and drainage basin characteristics. As the drainage area and thus water discharge increases, erosion rates intensify. Sudden increases in drainage area, such as through stream capture in the headwaters, can rapidly increase the rate of vertical erosion and abandon straths (García and Mahan, 2014). Rapid changes to river slope can occur locally from tectonic offset or base level fall (Gardner, 1983; García et al., 2004) and result in upstream propagating knickpoints or locally steepened zones where erosion is enhanced. Time transgressive strath terraces are formed as a result of the upstream propagation of knickpoints (Schoenbohm et al., 2004; Harkins et al., 2007). Although knickpoints represent a transient and local change in slope, channel slope can be influenced more broadly by basin lithology and sediment supply.

Lithology affects channel slope through setting the channel erodibility. More resistant lithologies that are harder to erode require steeper

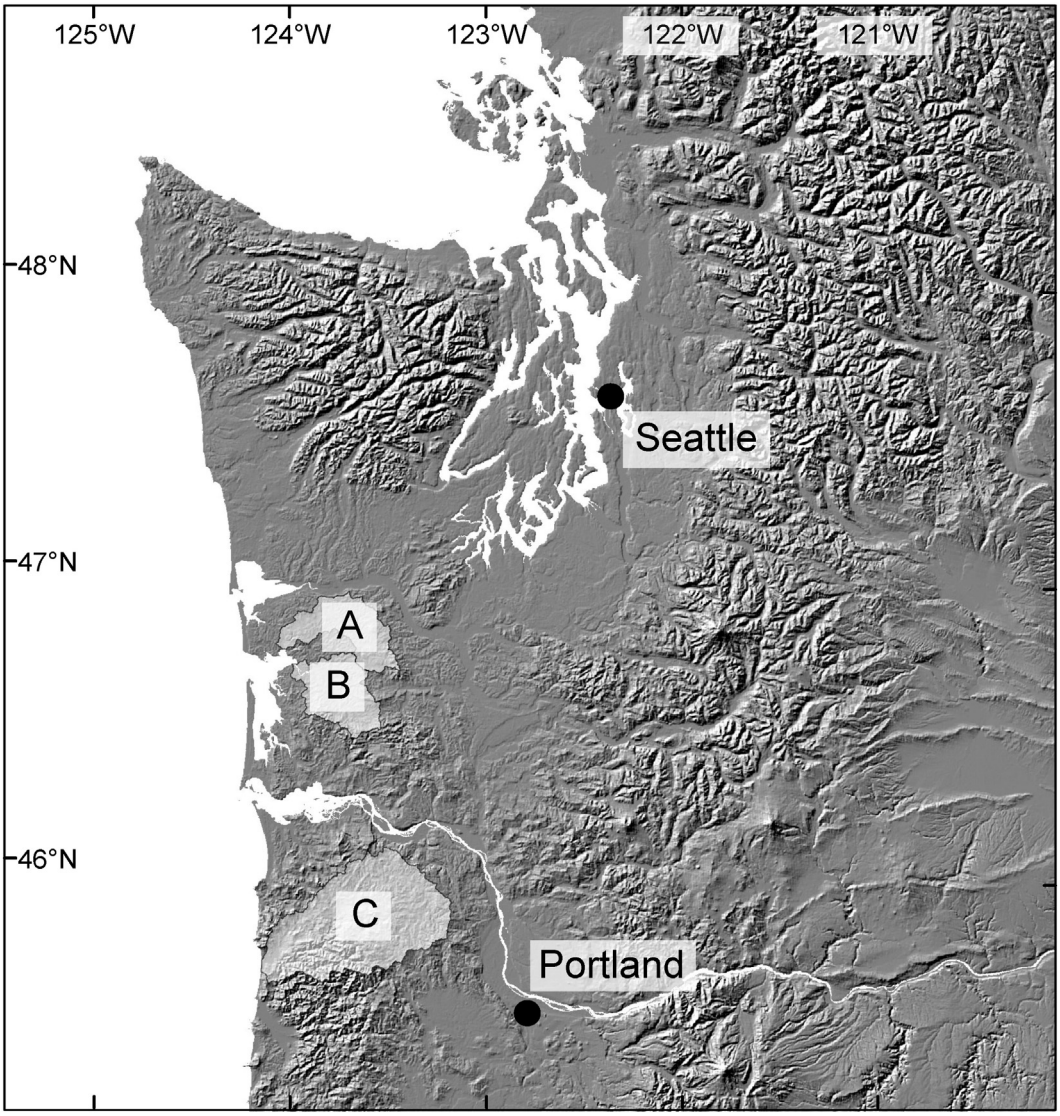

Fig. 1. Location of study basins in Washington and Oregon states. A is the North River, B is the Willapa River, and C is the Nehalem River.

channels to produce topographic equilibrium (Gilbert, 1877). For a channel with an equilibrium long profile, erosion and uplift rates will balance; thus, if an erosion resistant bedrock (low K in Eq. 1) and erosion susceptible bedrock (high K) with the same drainage area and uplift rate are compared, the erosion-resistant bedrock requires a steeper slope in order to balance the lower K value (Stock and Montgomery, 1999). In this way, steep erosion-resistant zones can persist and form long-lasting lithologic knickpoints (Cook et al., 2009).

The lithology and amount of sediment supply also influences channel slope and incision rates. In a study of actively uplifting streams in the Santa Ynez Mountains, Duvall et al. (2004) found streams in erosion-susceptible bedrock were steeper downstream of erosion-resistant bedrock reaches than in comparably sized streams where the entire basin was composed of the erosion-susceptible bedrock. They hypothesized that the transition in bedrock lithology resulted in a transport-limited system with a supply of highly durable bedload that effectively eroded and steepened the more readably eroded bedrock downstream. Abrasion-mill studies found erosion rate increases with the square of the tensile strength of the abrading material and is dependent on the supply of bedload material (Sklar and Dietrich, 2001). As bedload initially increases in supply, saltating and suspended grains are able to abrade the bedrock. However, as the supply continues to increase, the mobile bedload layer becomes shielded from bedrock by an underlying immobile bedload layer and erosion rates decline asymptotically to zero (Sklar and Dietrich, 2001; Turowski et al., 2007).

Building on previous work on channel slope, bedrock erodibility properties, and sediment supply, we investigate the formation of strath terraces in two distinct lithologies — an easily erodible siltstone and erosion-resistant basalt — through field mapping of strath terraces, radiocarbon dating to determine incision rates, valley width measurements, and longitudinal profile analysis, and we discuss the variables controlling rates of vertical and lateral erosion. In particular, we investigate how the previously discussed erosional mechanisms interact with lithology to determine valley width and thereby the potential for strath terrace formation and preservation.

3. Study areas

3.1. Willapa River

The Willapa River is located in southwest Washington State and drains an area of 680 km^2, flowing from the coastal Willapa Hills to Willapa Bay in the Pacific Ocean (Figs. 1, 2A). The basin has a temperate coastal maritime climate and can receive up to 3 m of precipitation per year, mainly in the form of rain (Owenby and Ezell, 1992). Pleistocene glaciation did not reach the Willapa River basin, and snow accumulation is only temporary in the highest peaks. The bedrock is composed of Eocene Crescent Formation basalt flows in the south and southwest upper watershed, and Eocene to Miocene marine sedimentary rocks in the main valley and northeast quadrant of the watershed (Walsh et al., 1987). The marine sedimentary rocks are primarily composed of the McIntosh and Lincoln Creek Formations and are a mix of siltstones, mudstones, and sandstones with conglomerate lenses. The sedimentary rocks are not heavily cemented and are easily friable when dry (Rau,

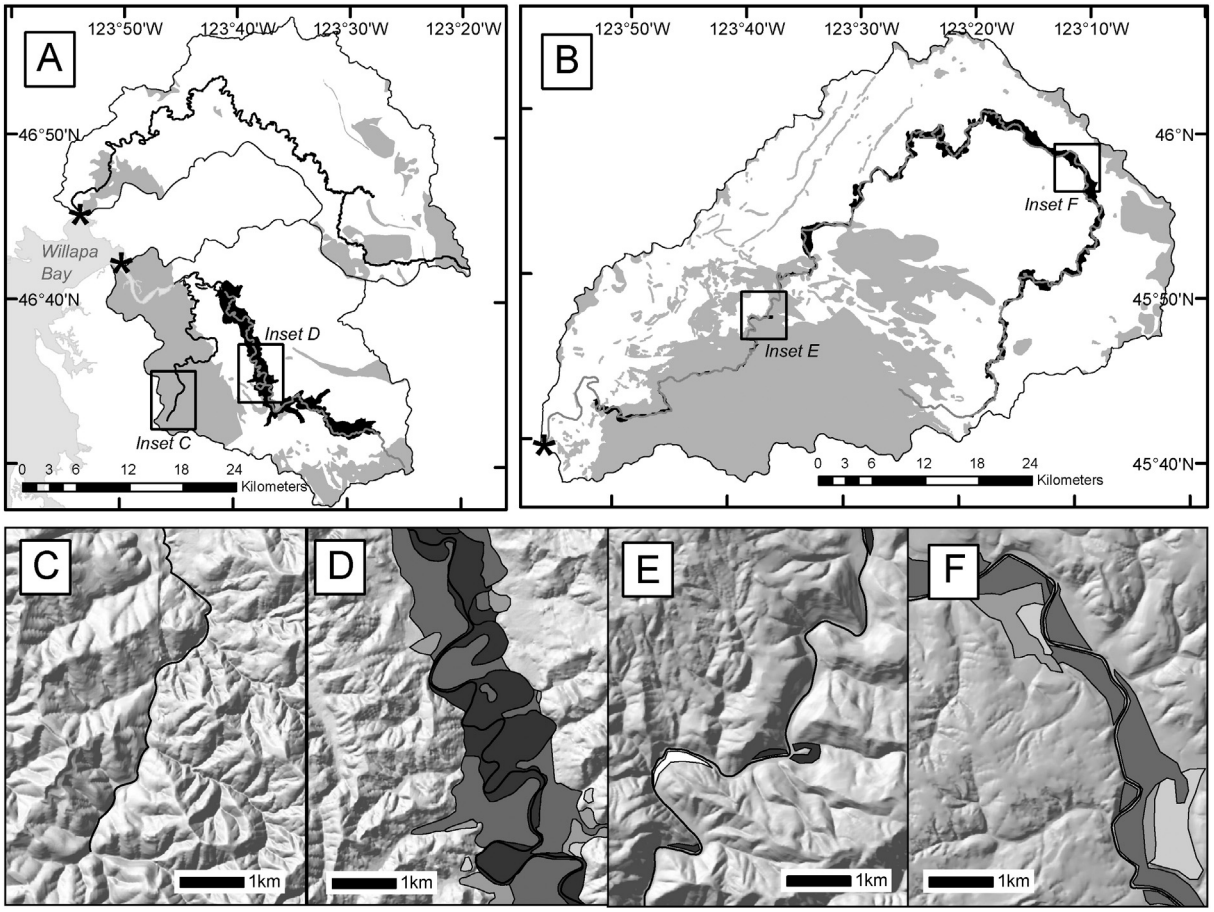

Fig. 2. Maps of geology and terraces of the (A) Willapa and North rivers, Washington, and (B) Nehalem River, Oregon, with basalt bedrock in gray and siltstone in white, and the extent of mapped fluvial terraces shown in black; asterisks mark river mouths. Boxes indicate locations of closer views of terraces located in typical basalt (C, E) and sandstone reaches (D, F), with a 10-m-grid DEM hillshade background. Terraces are shaded lighter for older age. North is up for all panels.

1951). The Crescent Formation basalts are fine-grained, resistant to erosion, and form pillows and block-jointed structures. The basin was logged and splash-dammed in the late 1800s (Wendler and Deschamps, 1955), and as a result the river lacks in-channel woody debris and is mostly bedrock-floored with a thin alluvial cover.

3.2. Nehalem River

The Nehalem River is located on the north coast of Oregon and drains from the Oregon Coast Range to the Pacific Ocean, discharging into Nehalem Bay (Figs. 1, 2B). It has a drainage area of 2210 km^2 and an average annual rainfall of 2.9 m but can receive up to 4.5 m of rain in its headwaters (Maser, 1999). Bedrock is mostly marine sedimentary rocks of middle Miocene to late Eocene age, with late to middle Eocene basalt in the lower 50 km as well as the headwaters above river kilometer (rkm) 197. The river valley was settled and logged in the late 1800s, and log drives and in-stream gravel mining cleared the channel of woody debris (Maser, 1999). The present channel is bedrock-floored with variable alluvial cover and lacks woody debris.

4. Methods

4.1. Mapping and incision rates

We mapped the spatial extent of terraces in the field onto 1:24,000 USGS topographic maps of the Nehalem and Willapa rivers. Mapping of terrace surfaces on the Nehalem River was supplemented by lidar using the DOGAMI Lidar Viewer (http://www.oregongeology.org/dogamilidarviewer/). Terrace surfaces were differentiated based on degree of soil development, basalt weathering rind thickness, and height above the river channel. Soil development was determined by visual observation and by comparing the depth of the B horizon and degree of clay alteration in buried alluvial cobbles. Basalt clasts in the preserved terrace alluvium were broken open and the weathering rind thickness used to correlate terraces across the study area. Lastly, terrace tread height above the current river channel was used to correlate terraces; the heights are given in Table 1. Charcoal samples were collected from within alluvium overlying straths and dated using accelerated mass spectrometry at Direct-AMS in Seattle, Washington (Table 2). Radiocarbon ages were calibrated using the methods developed by Stuiver and Reimer (1993) with the software Calib Rev. 7.0.2. Because of fluctuations in the global carbon reservoir over time, several radiocarbon ages contain multiple solutions when calibrated. We report all calibrated radiocarbon ages as 2σ ranges in calibrated years before present (cal YBP) for a probability > 0.25. Radiocarbon dates provide an estimate of the last time the strath was active, and incision rates obtained from these dates are minimum rates, as the true age of strath terrace abandonment could post-date the radiocarbon sample deposition. Incision rates are calculated using the midpoint of the 2σ calibrated age BP range and the height of the strath above the low flow water surface. The riverbed is mostly bedrock with a thin alluvial cover, and we interpret the bed fluctuations to be negligible as there is no indication of large, localized aggradation that could result in rapid changes to the riverbed elevation (Gallen et al., 2015).

Table 1
List of terraces.

Terrace	Elevation of terrace tread above river channel (meters)	Bedrock
Willapa T1	1–2	Siltstone
Willapa T2	3–6	Siltstone
Willapa T3	12–15	Siltstone
Willapa T4	20–25	Siltstone
Nehalem T1	<5	Basalt/shale
Nehalem T2	6	Shale
Nehalem T3	12	Shale
Nehalem T4	30	Shale
Nehalem T5	50	Shale

4.2. Valley width

We measured valley width as a constraint on the total lateral erosion and to characterize the space available for strath planation and preservation. To compare the influence of local lithology, we measured valley width versus upstream drainage area for locations underlain by basalt and marine sedimentary rocks. We include in this analysis data from the North River, which shares the same bedrock lithology and climate as the Willapa River and is located just north of the Willapa basin (Figs. 1 and 2). Drainage area provides a reasonable proxy for discharge, as the study basins receive comparable mean annual rainfall.

Drainage area was determined using the Hydrology toolset in ArcGIS. A 10-m-grid resolution DEM was used as the base layer, and flow accumulation was determined for each 10 × 10 m cell. The drainage area at each valley width measurement point was taken from the flow accumulation raster and converted to square kilometers.

In order to measure valley width and observe weathering behaviors in basalt and siltstone, field visits to each site were made. Heavy foliage in the tributary valleys prevented accurate field measurements of valley width, and the larger mainstem valleys were too wide to measure with our laser rangefinder. As a result, valley width was measured remotely from digital elevation models (DEMs), with field checks of valley width made where the line of sight was clear and valleys were narrow enough. Valley width was measured every 5 km along the channel for drainage areas >100 km^2, every 1 km for drainage areas between 10 and 100 km^2, and every 100 m for drainage areas <10 km^2. Measurements were made using the Measure tool in ArcGIS on 1:24,000 topographic maps, avoiding tributary junctions. We then checked valley width measurements for accuracy against any available finer resolution, lidar-derived DEMs.

4.3. Longitudinal stream characteristics

In order to assess the effect of lithology on channel steepness in our study sites, we constructed longitudinal profiles and conducted a slope-drainage area analysis to determine the steepness index and concavity values. Longitudinal profiles for the Nehalem, North, and Willapa rivers were created using 1:24,000 topographic maps to avoid inaccurate interpolations in the 10-m DEM. The maps were digitized in ArcGIS and distances and elevations extracted manually at the intersection of the river and contour lines. Using the line segments from the longitudinal profile, the slope-drainage area plot was constructed by calculating the slope of each line segment, spanning the stream distance between contour lines, and by obtaining the drainage area at the midpoint of each line using the same process as for the valley width versus drainage area plots. A power law regression of the form $S = k_s A^{\theta}$ was fit to the slope-drainage area plots, where k_s is the channel steepness index and θ is the concavity value.

5. Results

5.1. Field mapping and observations

Field mapping within the mainstem Willapa River identified four distinct strath terrace levels (Table 1, Fig. 2). The oldest terraces, T4 and T3, display a high degree of weathering on buried alluvial cobbles overlying the strath (Fig. 3A) and well-developed soil, while younger terraces T2 and T1 have little to no weathering rinds on alluvial cobbles (Fig. 3B) and are overlain by poorly developed soils. Five terraces were noted in the Nehalem River valley. In both basins, older terraces are preserved as unpaired and laterally discontinuous remnants, and T2 forms the main valley surface. The youngest terrace is inset into T2.

Table 2
Radiocarbon ages.

Sample ID	^{14}C age ($\pm 1\sigma$)	Calibrated age (2σ)[a]	Incision rate (mm/y)[b]	Latitude/longitude of sample (NAD 27)	Terrace
D-AMS 003607	68 ± 21	NA		46.5614/−123.612	T2
D-AMS 003606	94 ± 27	23–142 (0.73)	31.52	46.6104/−123.641	T1
		219–264 (0.27)	10.77		
D-AMS 011300	207 ± 24	146–189 (0.48)	7.58	46.6128/−123.638	T1
		268–301 (0.32)	4.46		
D-AMS 003604	219 ± 29	145–214 (0.5)	8.91	46.5341/−123.458	T1
		268–307 (0.4)	5.57		
D-AMS 005633	2918 ± 75	2862–3252	0.79	46.5562/−123.610	T2
D-AMS 007611	5962 ± 21	6734–6809	0.30	46.5354/−123.481	T2
D-AMS 011301	6765 ± 35	7576–7669	0.26	46.6288/−123.697	T2
D-AMS 005631	7909 ± 45	8598–8809	0.37	46.5815/−123.624	T2
D-AMS 005630	8896 ± 36	9904–10,179	0.20	46.5352/−123.481	T2
D-AMS 005632	8967 ± 34	10,122–10,227	0.13	46.5792/−123.626	T2
D-AMS 003603	9398 ± 47	10,512–10,736	0.16	46.5635/−123.566	T2
D-AMS 007612	9837 ± 27	11,204–11,265	0.31	46.5546/−123.608	T2

[a] Years before present, calibrated based on Stuiver and Reimer (1993) using CALIB REV 7.0.1.
Parentheses indicate *p*-value for samples returning more than one calibrated age.
[b] Calculated using height above low flow strath and midpoint of calibrated age.

The marine sedimentary rocks in both basins displayed visible evidence of ongoing rapid physical weathering within the high and low flow channels. In the Willapa basin, large talus piles several meters high accumulate annually on the eroding banks of the river, indicating rapid physical weathering of the siltstone (Fig. 4A). The bedrock is heavily fractured and slaking in centimeter-sized chunks from natural wetting and drying processes. The high flow channel banks contain 1–3 m high bedrock outcrops that are wetted during winter high flows and dry during summer low flow; this subaerially exposed bedrock has a high fracture density and is easily eroded. Fractured pieces of bedrock are easily removed by hand. Spheroidal weathering around concretions within the bedrock produces 5- to 10-mm thick rinds that readily peel off within the high flow channel bounds (Fig. 4B). A low flow bench is common in both basins, with a deeper low flow channel incised into bedrock. Bedrock subaqueously exposed within the low flow channel is resistant to erosion and does not contain the closely spaced fracture network that has developed in the subaerially exposed siltstone.

In contrast, basalt bedrock reaches have rougher beds, with resistant blocks of bedrock forming knobs that protrude from the low flow water surface. The original fracture density of the bedrock controls channel bedforms, such as the spacing of pools and riffles (Fig. 4C). Notably, a secondary, weathering produced fracture system, such as observed in the marine sedimentary bedrock, has not developed. Active weathering of channel basalt is not evident, and erosion appears to concentrate along the preexisting fractures in the basalt and takes the form of large block erosion from entrainment in large floods. During field visits, the subaerial and subaqueous basalt were equally resistant to erosion and could not be dislodged by hand or hammer (Fig. 4D).

5.2. Terrace ages and incision rates

Radiocarbon ages are reported in Table 2 and Fig. 5A. Calibrated ages range from 23 to 307 cal YBP for T1 and from 2862 to 11,265 cal YBP for T2, a span of almost 10,000 years. Sample D-AMS 003607 is not used further in our analysis; we believe the young age of this sample is because of contamination by recent flood debris. The subdued morphology of the terrace at this site, its height 3.5 m above the river bed and within reach of recent flooding, and the developed soil cover on the terrace all support an older age for this surface.

The rate of vertical bedrock incision is an order of magnitude lower for T2 terraces (Table 3, Fig. 5B), which is expected owing to the incorporation of multiple cycles of nonincision and incision with greater terrace age (Finnegan et al., 2014). Rates vary between 0.13 and 0.79 mm y^{-1} for T2 with a mean of 0.32 mm y^{-1}, while T1 incision rates are between 4.46 and 31.52 mm y^{-1} with a mean of 11.47 mm y^{-1}. Longitudinally, T1 incision rates are highest closer to the estuary (Fig. 5B); however, the three data points do not provide robust support for inferring a trend. Likewise, the incision rates from T2 are variable and do not show a statistically significant trend with upstream distance (Kendall's τ of −0.098, *p*-value of 0.88, with a sample size of 7).

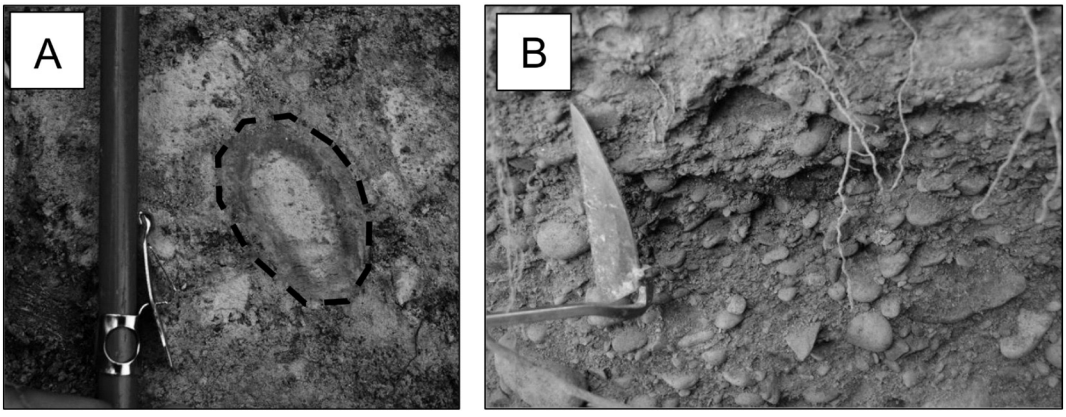

Fig. 3. (A) Weathered siltstone cobble from the Willapa River terrace T4 showing weathering rind and complete alteration to clay. Dashed line shows outer limit of cobble. (B) Siltstone and basalt cobbles in the alluvium overlying the strath of terrace T2 display intact cobbles and very little to no clay alteration.

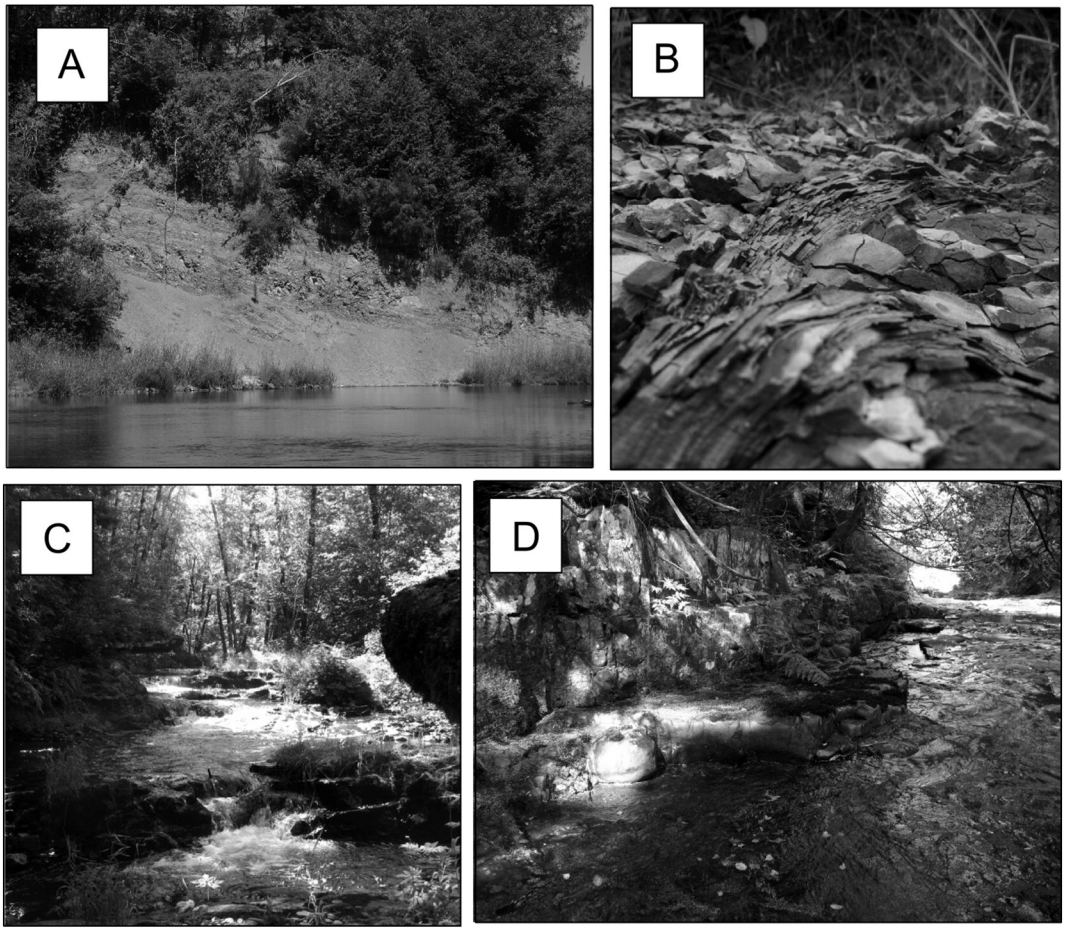

Fig. 4. (A) Talus piles accumulated on a 5-m high bank of the Willapa River, within the marine sedimentary bedrock. (B) Active weathering of subaerially exposed siltstone banks in 0.5–1.0 cm flakes. Siltstone within the active channel displayed none of the exfoliation weathering that is prevalent along the exposed banks and high flow channels. (C) Small knickpoint on Falls Creek, a tributary to the Willapa River, with basalt bedrock. Preexisting fractures in the basalt control erosion and determine knickpoint spacing and location. (D) Basalt bank on Falls Creek. Bank has blocky shape determined from preexisting fractures in the basalt where erosion concentrates. Flow is to the right.

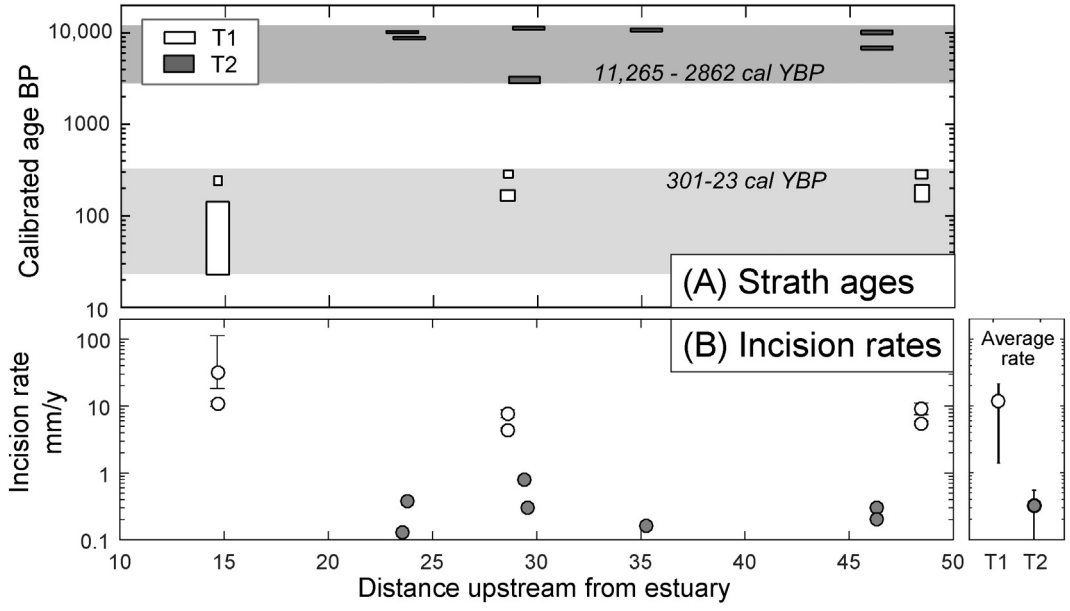

Fig. 5. (A) Calibrated ages for radiocarbon samples collected along the Willapa River. Gray bars indicate the minimum range of occupation times for T2 and T1 implied by the samples. Boxes show 2σ range of ages, and width of boxes corresponds to the age probability for samples returning multiple calibrations with a probability >0.25. (B) Incision rates calculated from the median calibrated age and strath height above low flow shown against distance upstream of the estuary for the Willapa River. Error bars show 2σ range of incision rates. White circles are T1, gray circles are T2. For both plots, data is shown for all age probabilities >0.25.

Table 3
Power law regression $w = bA^c$.

Bedrock	b (1σ)	c (1σ)	R^2
Marine sedimentary	67.1 ± 1.12	0.34 ± 0.03	0.45
Basalt	28.4 ± 1.09	0.22 ± 0.03	0.40

5.3. Valley width

Changes in valley width along the profile of the Nehalem and Willapa rivers reflect lithologic differences (Fig. 6). The widest valleys on the Nehalem River occur in the middle of the longitudinal profile (Fig. 6A), whereas the narrowest valleys are located at the farthest distance upstream from the outlet and in the reach immediately upstream of the outlet where the river is flowing through basalt. The longitudinal profile is steeper in the reaches underlain by basalt, coinciding with the narrower valleys. Profiles in the marine sedimentary rock are concave upward. In the South Fork of the Willapa River, a similar trend of narrower and steeper valleys in basalt bedrock is observed (Fig. 6B). Here, the valley width in basalt reaches is consistently <100 m, and a considerable widening is observed when the river encounters marine sedimentary bedrock where valley widths range from 300 to 900 m. The longitudinal profile shows abrupt breaks in slope at the transition between marine sedimentary and basalt bedrock valleys, with a concave up profile in marine sedimentary rock. The lower basalt reach is convex up, similar to the lower reach of the Nehalem River; while the upper basalt reach on the South Fork Willapa River is concave up but contains several sharp breaks in slope (e.g., at river kilometers 23 and 31).

When valley width is plotted against drainage area rather than longitudinal distance upstream, basalt and sedimentary bedrock valleys separate distinctly (Fig. 7). Basalt bedrock valleys are narrower than sedimentary bedrock valleys with the same drainage area. A power law least squares regression characterizes the behavior of each lithology with increasing drainage area. For both lithologies, as drainage area increases and the channel becomes larger, the valley width also increases. However, the width of sedimentary bedrock valleys increases with drainage area by a power of 0.34 ± 0.03, while basalt valleys increase by a power of 0.22 ± 0.03, indicating thtat the dependence of valley width on drainage area is not the same for all rock types (Table 3, Fig. 7). Although sedimentary valleys and basalt valleys widen as drainage area increases, sedimentary valleys are 2 to 3 times wider for the same drainage area. As drainage area continues to increase, the difference in width between basalt and sedimentary valleys increases; hence the influence of lithology on valley width appears to be greater at larger drainage areas.

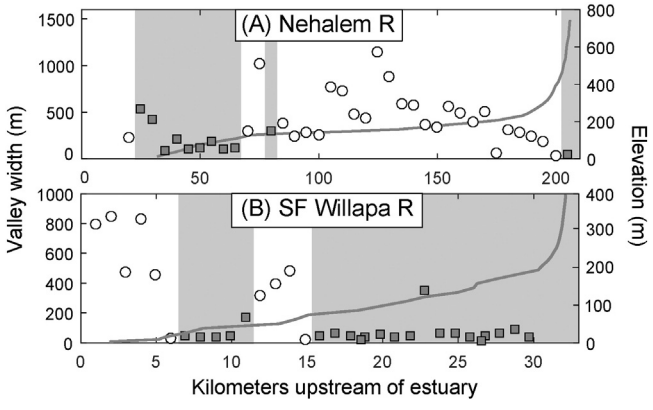

Fig. 6. Valley width and elevation as a function of distance upstream of the estuary for the (A) Nehalem and (B) South Fork Willapa rivers. Gray squares indicate valley width measured in basalt bedrock while white circles show marine sedimentary bedrock. The longitudinal profile is shown in dark gray, with regions underlain by basalt indicated by the shaded background. Distance is measured in kilometers from estuary, as determined along channel centerline; valley width is measured from 1:24,000 USGS topographic maps.

5.4. Slope-area analysis

For all three basins, the concavity (θ) and steepness indexes (k_s) are significantly different in basalt and sedimentary bedrock reaches (Fig. 8). In basalt, k_s values range from 0.07 to 0.18, while the corresponding values in sedimentary bedrock are from 0.22 to 0.32. For a given basin, the sedimentary bedrock k_s values are nearly double those in basalt. The concavity of sedimentary bedrock reaches is relatively consistent between watersheds, at 0.88, 0.94, and 0.96 for the Nehalem, North, and Willapa rivers, respectively. Concavity ranges more widely for the basalt reaches, at values of 0.42, 0.28, and 0.75 for those same rivers. When data from all three basins are combined, the k_s values are 0.27 and 0.16 and concavity values are 0.93 and 0.51 for the sedimentary and basalt bedrocks, respectively (Fig. 8D).

6. Discussion

6.1. Strath occupation time

Radiocarbon estimates of strath terrace ages span a wide range, indicating occupation of straths for extensive periods of time (Table 2, Fig. 5A). Calibrated radiocarbon ages for T2 have a range of nearly 10,000 years from 2862 to 11,265 cal YBP. This suggests T2 was an active valley floor experiencing deposition and lateral movement during most of the Holocene and, furthermore, because radiocarbon ages provide a minimum range, implies the occupation time could be even longer. The maximum duration of incision to abandon T2 interpolated from the calibrated ages is ~2500 years; this value is one-fourth of the minimum planational phase and supports previous studies that find planation periods much longer than incisional phases (Hancock and Anderson, 2002; Wegmann and Pazzaglia, 2002; Collins et al., 2016).

The long occupation time suggested by this study and others calls for caution in evaluating incision rates, especially those obtained from a single radiocarbon sample. Although incision rates obtained from T2 seem to cluster in comparison to T1 (Fig. 5B), they still span nearly an order of magnitude. The range in incision rates is caused by how much of the planation phase is encapsulated in the age; a greater ratio of time spent in planation than incision results in a lower apparent incision rate owing to the Sadler effect (Finnegan et al., 2014). That inferred incision rates can vary greatly depending on sample location calls for care in using incision rates to infer rates of tectonic rock uplift. Previous authors have suggested using incision rates from terraces spanning a full glacial cycle (Wegmann and Pazzaglia, 2002) or using the lowest terrace as the reference frame to calculate incision (Gallen et al., 2015). However, if terraces can be active for up to 10,000 years, as our radiocarbon dates show, then using either of these methods without taking into account the full range of terrace occupation would still result in erroneous uplift rates.

Additionally, the relative time spans of the two terrace sets observed on the Willapa River indicates a recent shift in river incision rates. Terrace T2 is the Holocene strath terrace and was active for nearly 10,000 years before significant incision occurred to abandon it. Average incision rates are close to the long-term exhumation rates reported in the Olympic Mountains (Brandon et al., 1998). The lower terrace, T1, is much more restricted in areal extent (Fig. 2D) and the strath was occupied for less time, possibly up to 300 years. Incision and terrace abandonment initiated only in the last hundred years, and incision rates are much higher than short-term geodetic uplift rates that measure between 0.4 and 0.8 mm y^{-1} (Pazzaglia and Brandon, 2001). The recent abandonment of T1 falls within the Anthropocene and may well indicate an anthropogenic influence on the landscape, which may also explain why incision rates are two orders of magnitude higher than

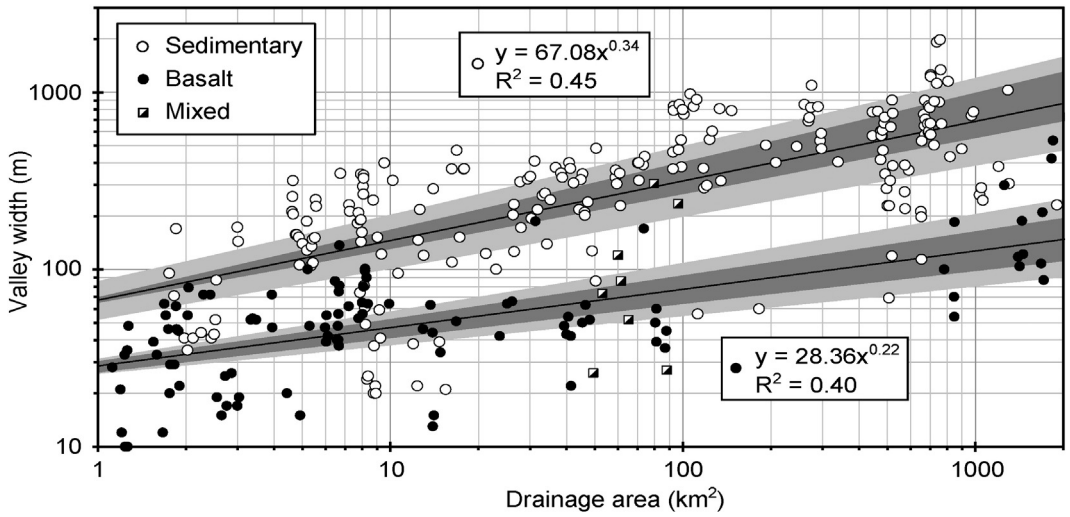

Fig. 7. Drainage area versus valley width data for the Nehalem, Willapa, and North rivers. Open circles indicate marine sedimentary bedrock and closed circles denote basalt bedrock. Half-filled squares specify locations at the transition between marine sedimentary and basalt bedrock. Light gray shading shows 2σ standard error of the power law regression and dark gray shading shows 1σ standard error. Exponents of the regression and 1σ errors are found in Table 3.

geodetic uplift rates. Recently, Collins et al. (2016) suggested in-stream wood loss can trigger incisional periods in a river through the removal of stored accumulations of sediment once held in place by log jams; historical documents show the Willapa River was logged and cleared of wood around the time T1 incision initiated. Further evidence is needed to link the two events, but the correlation between wood loss and incision in the Willapa River and the West Fork Teanaway River (Collins et al., 2016) suggests fluvial wood is a currently underestimated control on river incision.

6.2. Lithological control on valley width

Our finding that valley width, and thus strath terrace development, is controlled by lithologic variation within individual watersheds establishes that lithology is indeed a primary control on strath terrace formation, as suggested by previous work based on a compilation of studies in which straths were reported in various lithologies (Montgomery, 2004). We found little to no strath terrace development in basalt bedrock in the Willapa and Nehalem basins and multiple flights of well-developed strath terraces in sedimentary bedrock in both basins (Fig. 2). Observations on erosional style suggest rapid weathering by slaking is responsible for the widening and formation of straths in sedimentary bedrock. This observation is supported by measurements in similarly friable bedrock such as the Roslyn Formation in the central Cascade Range (Collins et al., 2016) and the Lincoln Creek Formation in the southern Olympic Mountains (Stock et al., 2005).

In contrast, basalt and more resistant lithologies that are not subject to weathering by slaking are slower to erode, forming narrower valleys.

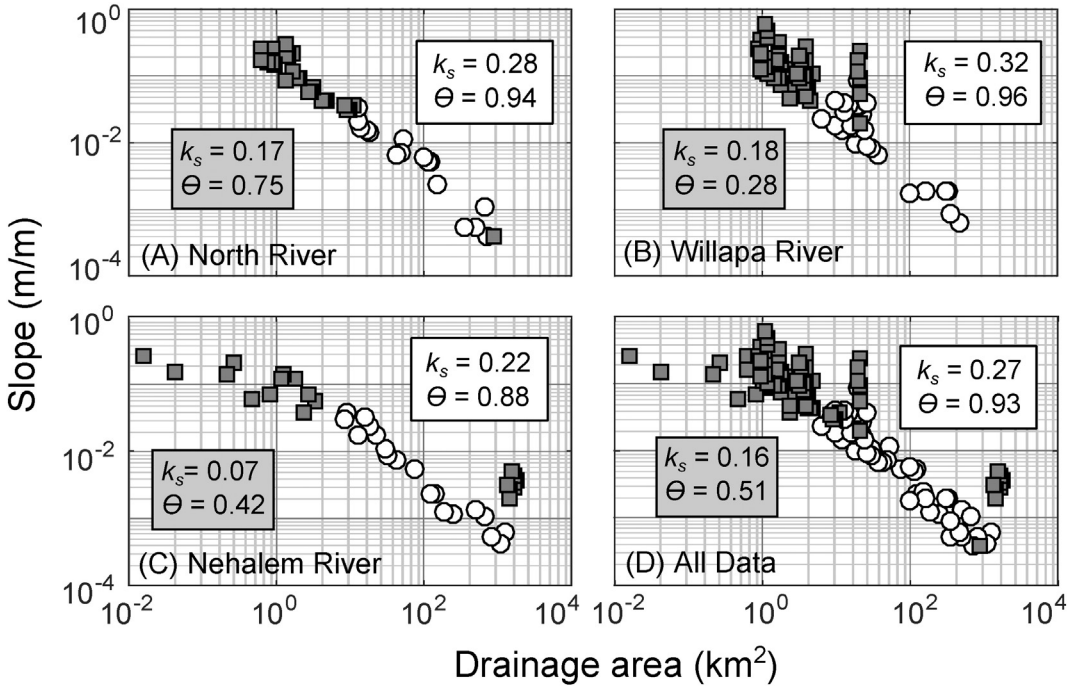

Fig. 8. Slope-area plots for the (A) North River, (B) Willapa River, (C) Nehalem River, and (D) all rivers. All plots are to the same scale. Gray squares are basalt bedrock and white circles represent marine sedimentary bedrock. Steepness indexes (k_s) and concavity (θ) are shown in gray boxes for basalt and white boxes for the marine sedimentary bedrock.

Concavity values in the basalt-floored streams span a broad range (Fig. 8), suggesting erosional mechanisms vary widely; this is likely indicative of variations in the original fracture density that control the erosional style. These values fall nicely within the range of concavity values previously noted in a set of diverse landscapes and lithologies and imply that erosion is dependent on either shear stress or unit stream power (Tucker and Whipple, 2002). Channels eroding sedimentary bedrock, however, have very similar values of concavity because the original fracture patterns are overprinted by a new, dense, system of fractures caused by slaking. The concavity values obtained in these sedimentary basins are close to 1, a value previously only found in the Oregon Coast Range (Seidl and Dietrich, 1992). Seidl and Dietrich (1992) hypothesized streams with $\theta \sim 1$ erode based on total stream power with a strong dependence on discharge. Tucker and Whipple (2002) later dismissed the total stream power model based on a lack of streams with $\theta \sim 1$ and on a poor fit with modeled and observed topography. Our results indicate a θ of 1 is not an anomalous value but perhaps a value common to streams draining easily friable sedimentary rocks, such as those in our study and that of Seidl and Dietrich (1992). Rapid slaking in these streams throughout the dry season unravels the bedrock such that sand-sized particles are produced and easily washed downstream. Thus, for these channels erosion is not dependent on unit stream power but instead on having a wet and dry season and a flow sufficient to transport sand-sized particles. It follows that streams draining such friable rocks would have erosion rates dependent on discharge, or drainage area in Eq. (1); and thus we infer that the total stream power model of Seidl and Dietrich (1992), in which $m = n = 1$ (Eq. 1) and producing $\theta \sim 1$, is applicable to a subset of bedrock mountain rivers where the bedrock lithology is prone to rapid slaking.

Channel erosion properties appear to scale up to control the valley width in the friable sedimentary bedrock. The width of valleys increases with drainage area at a similar rate as the stream channel width in sedimentary-floored streams. Montgomery and Gran (2001) found channel width along the sedimentary bedrock channels of the Willapa River increased with drainage area in a power law relationship where the exponent is 0.32 ± 0.02, within error of the exponent we find for valley width and drainage area in the same bedrock (Table 3, Fig. 7). This suggests that erosional processes controlling channel width also apply to valley width and implies a dependence on channel width for lateral channel migration. Rearranging the equation obtained by Montgomery and Gran (2001) and the relationship between drainage area and valley width given in this study, we find that valley width is 14.4 times the channel width for all drainage areas in the sedimentary bedrock.

Hence, lateral erosion by the channel appears to scale with the original width of the channel. We suspect that this scaling reflects an indirect link between channel and valley width through meander amplitude. The relationship between meander amplitude and channel width is also linear but varies with individual channels where meander amplitude can be 2.4 to 18.6 times the channel width (Leopold et al., 1964, and references therein). Our relationship between valley width and channel width falls within that range and suggests that valley width is controlled by the meander amplitude.

The relationship between channel and valley width applies to the marine sedimentary bedrock that is prone to slaking but does not hold true for basalt bedrock where erosion is unsteady and dependent on original fracture patterns. In the following sections, we further explore the mechanisms by which lithological differences control lateral and vertical erosion and thus strath formation: channel steepness and planform, channel versus bedload lithology, and bedrock mineralogy.

6.2.1. Channel steepness and planform

As previously discussed, more resistant lithologies form steeper channels. As a result, stream power — the product of water surface slope, flow depth, water density, and gravitational acceleration — is increased and vertical erosion enhanced. Increased vertical erosion will diminish the likelihood of long periods of lateral planation that are required to form straths; even if lateral planation is occurring, rapid vertical erosion will result in a sloped surface rather than the formation of a planar terrace (Merritts et al., 1994).

A secondary effect of steepened channels is a shift in channel planform. The Nehalem River is a meandering, single-thread channel that rapidly transitions to a much less sinuous, near straight channel where the bedrock shifts to basalt (Fig. 2). The South Fork Willapa River follows a similar trend as it comes in and out of the basalt and sedimentary bedrock; the basalt channels are less sinuous than the sedimentary bedrock channels. Straight planforms allow less lateral erosion and planation than braided or meandering channels, which are much more laterally mobile with continuous bank erosion and creation. Finnegan and Balco (2013) argued that braided channels are more likely to plane straths than other planforms, as the disorderly and dynamic nature of the braided channel allows it to rapidly widen a valley and erode a planar bedrock surface. If lithology exerts a first-order control on channel steepness, then channel planform will also depend on lithology, and thus the potential for planation is dependent on bedrock strength.

6.2.2. Lithologic contrasts

The volume of sediment supplied to the channel affects rates of vertical incision, but the strength of the supplied sediment will also have a considerable effect on rates of channel erosion. In the Nehalem and Willapa rivers, competent basalt bedrock is eroded in the steep hillslopes and provides long-lasting, attrition-resistant bed material. Although the Willapa River is composed of sedimentary bedrock for tens of kilometers upstream, the dominant bedload material is basalt of cobble to gravel size. This indicates that the local bedrock is not the abrasive tool but rather that basalt bed material sourced from the headwaters is doing most of the geomorphic work. Additionally, the amount of bed material is limited owing to rapid attrition of the marine sedimentary bedrock, which makes up the majority of the basin. Any input of siltstone to the channel breaks down to sand-size particles when dry and so is rapidly transported out of the system in the next flood. As a direct result, the Nehalem and Willapa rivers are likely to remain mixed bedrock-alluvial and are unlikely to become fully alluvial unless an external sediment source is added or the retention of sediment on the riverbed is increased.

In a study of rivers draining the Oregon Coast Range, O'Connor et al. (2014) found attrition rates varied widely between different basin lithologies and was the main control on bed material transport rates and channel cover. Similarly, Duvall et al. (2004) found steeper channel reaches in erosion-susceptible rock where the bedload was comprised of erosion-resistant rock sourced upstream. Both these findings indicate the presence of competent upstream bed material combined with a mechanically weak bedrock prone to slaking results in less bed cover, steeper slopes, and thus greater incision rates. Studies in mechanically weak rock with competent bed material record rapid incision rates on the order of cm y^{-1}, much greater than background geologic erosion rates of 1 mm y^{-1} or less (Stock et al., 2005; Collins et al., 2016). Incision rates on the Willapa River are also unusually rapid for the last incision cycle, from T1 to present, while incision rates from T2 to present, which incorporate a period of nonincision, are an order of magnitude lower and are similar to long-term rock uplift rates reported by Brandon et al. (1998). Hence, as long as there is base level accommodation space, rivers such as the Nehalem and Willapa, composed of a majority of mechanically weak bedrock and a headwater source of erosion resistant bed material, are likely to be in incisional phases. However, our radiocarbon dates indicate that this is not the case, with planation of T2 occurring for most of the Holocene and suggesting that there must be a mechanism to slow vertical incision and favor lateral widening.

If mechanically weak rock with resistant bed material is susceptible to rapid rates of erosion caused by the strength differences in the bedload and bedrock, we would expect rivers in this situation to be

deeply incised with no terraces. However, rapid vertical incision creates steep bedrock banks perched above the water table and exposed to mechanical and chemical weathering processes. The marine sedimentary bedrock of the Willapa and Nehalem rivers has a high mica content and is prone to physical weathering from wetting and drying. As the bedrock banks become exposed and perched higher above the low flow channel, cycles of wetting and drying through the year mechanically loosen the bedrock (Figs. 4A, B). During high flows, the loosened material is rapidly transported away, resulting in up to centimeters of lateral erosion in one event (Montgomery, 2004; Stock et al., 2005; Collins et al., 2016). This process is noted not only on the Willapa and Nehalem rivers, applying to fluvial terraces, but has also been postulated to be the mechanism behind wave cut bench formation (Retallack and Roering, 2012). Collins et al. (2016) hypothesized that rapid lateral widening also occurs if a low bench of easily friable bedrock is exposed during an extreme flow event. The bench undergoes lateral and vertical erosion by slaking, as well as physical abrasion in high flows, and can erode laterally at rates of decimeters per year (Collins et al., 2016).

As rapid erosion of exposed bedrock banks proceeds, the channel widens and water flow depth as well as stream power is lowered, thus slowing rates of vertical incision. Additionally, the decrease in stream power will reduce the transport capacity of the stream and result in aggradation, further protecting the bed from erosion. The process of widening results in a negative feedback to the incising stream that will arrest incision and turn the system toward lateral planation. Gravel deposits on top of T2 straths in the Willapa basin indicate that when the strath was active, sufficient gravel was accumulated in the channel to promote planation and slow incision. Because competent gravel supply to the system was likely as low as it is today, this indicates that the transport capacity was much lower during T2 occupation in order to accumulate gravel. This could be accomplished through a shallower slope, wider channel, or the presence of woody debris jams that partition shear stress and trap sediment. The long occupation time of T2 indicates that these conditions were stable through most of the Holocene.

7. Conclusions

Erosional properties unique to each lithology control valley width and thus the potential for strath planation and preservation, with slaking-type erosion creating valleys 2–3 times wider in marine sedimentary bedrock than in the relatively erosion-resistant basalt. Concavity values indicate basalt is eroding consistent with unit stream power erosion models while the sedimentary rocks of the Willapa and Nehalem basins follow a total stream power model that relies primarily on discharge as the main erosive agent. In readably friable rocks that annually slake into sand-size pieces, the total stream power model can accurately depict erosion as erosion in slaking rocks is dependent on subaerial weathering rather than fluvial abrasion or plucking. Additionally, the difference in rock strength between bedload and bedrock in the Willapa and Nehalem rivers leaves them prone to rapid vertical incision, although widening of bedrock banks from slaking can slow this process by lowering the transport capacity. Accumulations of fluvial wood during the Holocene likely retained more sediment on the channel bed, slowing incision rates and leading to more lateral movement. The loss of this wood, and associated lowered sediment retention, possibly attributed to the rapid ongoing incision that is abandoning the lowest terrace.

Acknowledgments

This work was supported by the Department of Earth and Space Sciences and the Quaternary Research Center at the University of Washington and by a Geological Society of America Graduate Student Research Grant to S Schanz. The authors thank R Schanz, T Hillebrand, and A Pacubas for help with field work and L Nakonechny, J O'Connor, C Cannon, and H Bervid for useful discussions in the field. The editor and an anonymous reviewer provided useful revisions which improved the manuscript.

Appendix A. Supplementary data

Supplementary data associated with this article can be found in the online version at http://dx.doi.org/10.1016/j.geomorph.2016.01.015. These data include the Google maps of the most important areas described in this article.

References

Barnard, P.L., Owen, L.A., Sharma, M.C., Finkel, R.C., 2004. Late Quaternary (Holocene) landscape evolution of a monsoon-influenced high Himalayan valley, Gori Ganga, Nanda Devi, NE Garhwal. Geomorphology 61, 91–110. http://dx.doi.org/10.1016/j.geomorph.2003.12.002.

Brandon, M.T., Roden-Tice, M.K., Garver, J.I., 1998. Late Cenozoic exhumation of the Cascadia accretionary wedge in the Olympic Mountains, northwest Washington State. Geol. Soc. Am. Bull. 110, 985–1009. http://dx.doi.org/10.1130/0016-7606(1998)110<0985:LCEOTC>2.3.CO;2.

Cheng, S., Deng, Q., Zhou, S., Yang, G., 2002. Strath terraces of Jinshaan Canyon, Yellow River, and Quaternary tectonic movements of the Ordos Plateau, North China. Terra Nova 14, 215–224. http://dx.doi.org/10.1046/j.1365-3121.2002.00350.x.

Collins, B.D., Montgomery, D.R., Schanz, S.A., Larsen, I.J., 2016. Rates and mechanisms of bedrock incision and strath terrace formation in a forested catchment, Cascade Range, Washington. Geol. Soc. Am. Bull. B31340, 1. http://dx.doi.org/10.1130/B31340.1.

Cook, K.L., Whipple, K.X., Heimsath, A.M., Hanks, T.C., 2009. Rapid incision of the Colorado River in Glen Canyon — insights from channel profiles, local incision rates, and modeling of lithologic controls. Earth Surf. Process. Landf. 34, 994–1010. http://dx.doi.org/10.1002/esp.1790.

Duvall, A., Kirby, E., Burbank, D., 2004. Tectonic and lithologic controls on bedrock channel profiles and processes in coastal California. J. Geophys. Res. Earth Surf. 109, F03002. http://dx.doi.org/10.1029/2003JF000086.

Finnegan, N.J., Balco, G., 2013. Sediment supply, base level, braiding, and bedrock river terrace formation: Arroyo Seco, California, USA. Geol. Soc. Am. Bull. 125, 1114–1124. http://dx.doi.org/10.1130/B30727.1.

Finnegan, N.J., Dietrich, W.E., 2011. Episodic bedrock strath terrace formation due to meander migration and cutoff. Geology 39, 143–146. http://dx.doi.org/10.1130/G31716.1.

Finnegan, N.J., Schumer, R., Finnegan, S., 2014. A signature of transience in bedrock river incision rates over timescales of 104–107 years. Nature 505, 391–394. http://dx.doi.org/10.1038/nature12913.

Fuller, T.K., Perg, L.A., Willenbring, J.K., Lepper, K., 2009. Field evidence for climate-driven changes in sediment supply leading to strath terrace formation. Geology 37, 467–470. http://dx.doi.org/10.1130/G25487A.1.

Gallen, S.F., Pazzaglia, F.J., Wegmann, K.W., Pederson, J.L., Gardner, T.W., 2015. The dynamic reference frame of rivers and apparent transience in incision rates. Geology 43, 623–626. http://dx.doi.org/10.1130/G36692.1.

García, A.F., 2006. Thresholds of strath genesis deduced from landscape response to stream piracy by Pancho Rico Creek in the Coast Ranges of central California. Am. J. Sci. 306, 655–681. http://dx.doi.org/10.2475/08.2006.03.

García, A.F., Mahan, S.A., 2014. The notion of climate-driven strath-terrace production assessed via dissimilar stream-process response to late Quaternary climate. Geomorphology 214, 223–244. http://dx.doi.org/10.1016/j.geomorph.2014.02.008.

García, A.F., Zhu, Z., Ku, T.L., Chadwick, O.A., Chacón Montero, J., 2004. An incision wave in the geologic record, Alpujarran Corridor, southern Spain (Almería). Geomorphology 60, 37–72. http://dx.doi.org/10.1016/j.geomorph.2003.07.012.

Gardner, T.W., 1983. Experimental study of knickpoint and longitudinal profile evolution in cohesive, homogeneous material. Geol. Soc. Am. Bull. 94, 664–672. http://dx.doi.org/10.1130/0016-7606(1983)94<664:ESOKAL>2.0.CO;2.

Gilbert, G.K., 1877. Report on the Geology of the Henry Mountains. US Government Printing Office.

Hancock, G.S., Anderson, R.S., 2002. Numerical modeling of fluvial strath-terrace formation in response to oscillating climate. Geol. Soc. Am. Bull. 114, 1131–1142. http://dx.doi.org/10.1130/0016-7606(2002)114<1131:NMOFST>2.0.CO;2.

Hancock, G.S., Small, E.E., Wobus, C., 2011. Modeling the effects of weathering on bedrock-floored channel geometry. J. Geophys. Res. Earth Surf. 116, F03018. http://dx.doi.org/10.1029/2010JF001908.

Harkins, N., Kirby, E., Heimsath, A., Robinson, R., Reiser, U., 2007. Transient fluvial incision in the headwaters of the Yellow River, northeastern Tibet, China. J. Geophys. Res. Earth Surf. 112, F03S04. http://dx.doi.org/10.1029/2006JF000570.

Larson, P.H., Dorn, R.I., 2014. Strath development in small arid watersheds: case study of South Mountain, Sonoran Desert, Arizona. Am. J. Sci. 314, 1202–1223. http://dx.doi.org/10.2475/08.2014.02.

Lavé, J., Avouac, J.P., 2000. Active folding of fluvial terraces across the Siwaliks Hills, Himalayas of central Nepal. J. Geophys. Res. Solid Earth 105, 5735–5770. http://dx.doi.org/10.1029/1999JB900292.

Leopold, L.B., Wolman, M.G., Miller, J.P., 1964. Fluvial Processes in Geomorphology. W.H. Freeman, San Francisco.

Maser, J. 1999, Nehalem River Watershed Assessment: http://web.pdx.edu/~maserj/project/project1/ (Nov 2014).

Mériaux, A.-S., Tapponnier, P., Ryerson, F.J., Xiwei, X., King, G., Van der Woerd, J., Finkel, R.C., Haibing, L., Caffee, M.W., Zhiqin, X., Wenbin, C., 2005. The Aksay segment of the northern Altyn Tagh fault: tectonic geomorphology, landscape evolution, and Holocene slip rate. J. Geophys. Res. Solid Earth 110, B04404. http://dx.doi.org/10.1029/2004JB003210.

Merritts, D.J., Vincent, K.R., Wohl, E.E., 1994. Long river profiles, tectonism, and eustasy: a guide to interpreting fluvial terraces. J. Geophys. Res. Solid Earth 99, 14031–14050. http://dx.doi.org/10.1029/94JB00857.

Molin, P., Fubelli, G., Nocentini, M., Sperini, S., Ignat, P., Grecu, F., Dramis, F., 2012. Interaction of mantle dynamics, crustal tectonics, and surface processes in the topography of the Romanian Carpathians: a geomorphological approach. Glob. Planet. Chang. 90–91, 58–72. http://dx.doi.org/10.1016/j.gloplacha.2011.05.005.

Montgomery, D.R., 2004. Observations on the role of lithology in strath terrace formation and bedrock channel width. Am. J. Sci. 304, 454–476. http://dx.doi.org/10.2475/ajs.304.5.454.

Montgomery, D.R., Gran, K.B., 2001. Downstream variations in the width of bedrock channels. Water Resour. Res. 37, 1841–1846. http://dx.doi.org/10.1029/2000WR900393.

O'Connor, J.E., Mangano, J.F., Anderson, S.W., Wallick, J.R., Jones, K.L., Keith, M.K., 2014. Geologic and physiographic controls on bed-material yield, transport, and channel morphology for alluvial and bedrock rivers, western Oregon. Geol. Soc. Am. Bull. B30831, 1. http://dx.doi.org/10.1130/B30831.1.

Owenby, J.R., Ezell, D.S., 1992. Monthly Station Normals of Temperature, Precipitation, and Heating and Cooling Degree Days, 1961–1990: Washington. U.S. Department of Commerce, National Oceanic and Atmospheric Administration, National Climatic Data Center.

Pazzaglia, F.J., 2013. Fluvial terraces. Treatise on Geomorphology. Elsevier, pp. 379–412.

Pazzaglia, F.J., Brandon, M.T., 2001. A fluvial record of long-term steady-state uplift and erosion across the Cascadia forearc high, Western Washington state. Am. J. Sci. 301, 385–431. http://dx.doi.org/10.2475/ajs.301.4-5.385.

Personius, S.F., Kelsey, H.M., Grabau, P.C., 1993. Evidence for regional stream aggradation in the Central Oregon Coast range during the Pleistocene–Holocene transition. Quat. Res. 40, 297–308. http://dx.doi.org/10.1006/qres.1993.1083.

Rau, W.W., 1951. Tertiary foraminifera from the Willapa River Valley of Southwest Washington. J. Paleontol. 25, 417–453. http://dx.doi.org/10.2307/1299745.

Retallack, G.J., Roering, J.J., 2012. Wave-cut or water-table platforms of rocky coasts and rivers? GSA Today 4–10. http://dx.doi.org/10.1130/GSATG144A.1.

Schoenbohm, L.M., Whipple, K.X., Burchfiel, B.C., Chen, L., 2004. Geomorphic constraints on surface uplift, exhumation, and plateau growth in the Red River region, Yunnan Province, China. Geol. Soc. Am. Bull. 116, 895–909. http://dx.doi.org/10.1130/B25364.1.

Seidl, M.A., Dietrich, W.E., 1992. The problem of channel erosion into bedrock, in: Schmidt, K.-H., de Ploey, J. (Eds.), Functional Geomorphology: Landform Analysis and Models, Catena Supplement. pp. 101–124.

Sklar, L.S., Dietrich, W.E., 2001. Sediment and rock strength controls on river incision into bedrock. Geology 29, 1087–1090. http://dx.doi.org/10.1130/0091-7613(2001)029<1087:SARSCO>2.0.CO;2.

Snyder, N.P., Kammer, L.L., 2008. Dynamic adjustments in channel width in response to a forced diversion: Gower Gulch, Death Valley National Park, California. Geology 36, 187–190. http://dx.doi.org/10.1130/G24217A.1.

Stock, J.D., Montgomery, D.R., 1999. Geologic constraints on bedrock river incision using the stream power law. J. Geophys. Res. Solid Earth 104, 4983–4993. http://dx.doi.org/10.1029/98JB02139.

Stock, J.D., Montgomery, D.R., Collins, B.D., Dietrich, W.E., Sklar, L., 2005. Field measurements of incision rates following bedrock exposure: implications for process controls on the long profiles of valleys cut by rivers and debris flows. Geol. Soc. Am. Bull. 117, 174–194. http://dx.doi.org/10.1130/B25560.1.

Stuiver, M., Reimer, P.J., 1993. Extended 14C data base and revised CALIB 3.014 C age calibration program. Radiocarbon 35, 215–230.

Tucker, G.E., Whipple, K.X., 2002. Topographic outcomes predicted by stream erosion models: sensitivity analysis and intermodel comparison. J. Geophys. Res. Solid Earth 107, 2179. http://dx.doi.org/10.1029/2001JB000162.

Turowski, J.M., Lague, D., Hovius, N., 2007. Cover effect in bedrock abrasion: a new derivation and its implications for the modeling of bedrock channel morphology. J. Geophys. Res. Earth Surf. 112, F04006. http://dx.doi.org/10.1029/2006JF000697.

Turowski, J.M., Hovius, N., Meng-Long, H., Lague, D., Men-Chiang, C., 2008. Distribution of erosion across bedrock channels. Earth Surf. Process. Landf. 33, 353–363. http://dx.doi.org/10.1002/esp.1559.

Van der Woerd, J., Ryerson, F.J., Tapponnier, P., Gaudemer, Y., Finkel, R., Meriaux, A.S., Caffee, M., Guoguang, Z., Qunlu, H., 1998. Holocene left-slip rate determined by cosmogenic surface dating on the Xidatan segment of the Kunlun fault (Qinghai, China). Geology 26, 695–698. http://dx.doi.org/10.1130/0091-7613(1998)026<0695:HLSRDB>2.3.CO;2.

Walsh, T.J., Korosec, M.A., Phillips, W.M., Logan, R.L., Schasse, H.W., 1987. Geologic Map of Washington, Southwest Quadrant [Map]: Washington Division of Geology and Earth Resources, Scale 1:100,000, 1 Sheet.

Wegmann, K.W., Pazzaglia, F.J., 2002. Holocene strath terraces, climate change, and active tectonics: the Clearwater River basin, Olympic Peninsula, Washington State. Geol. Soc. Am. Bull. 114, 731–744. http://dx.doi.org/10.1130/0016-7606(2002)114<0731:HSTCCA>2.0.CO;2.

Wegmann, K.W., Pazzaglia, F.J., 2009. Late Quaternary fluvial terraces of the Romagna and Marche Apennines, Italy: climatic, lithologic, and tectonic controls on terrace genesis in an active orogen. Quat. Sci. Rev. 28, 137–165. http://dx.doi.org/10.1016/j.quascirev.2008.10.006.

Wendler, H.O., Deschamps, G., 1955. Logging dams on coastal Washington streams. Washington Department of Fisheries, Fisheries Research Papers 1, 27–38.

Wohl, E., 2008. The effect of bedrock jointing on the formation of straths in the Cache la Poudre River drainage, Colorado Front Range. J. Geophys. Res. Earth Surf. 113, F01007. http://dx.doi.org/10.1029/2007JF000817.

Yanites, B.J., Tucker, G.E., 2010. Controls and limits on bedrock channel geometry. J. Geophys. Res. Earth Surf. 115, F04019. http://dx.doi.org/10.1029/2009JF001601.